

Inspection of aluminum alloys by a multi-frequency eddy current method

A.V. EGOROV^a, V.V. POLYAKOV^{a,b}, D.S. SALITA^a, E.A. KOLUBAEV^{b,c,*}, S.G. PSAKHIE^{b,c},
A.G. CHERNYAVSKII^d, I.V. VOROBEL^d

^a Altai State University, Russia

^b Institute of Strength Physics and Materials Science SB RAS, Russia

^c National Research Tomsk Polytechnic University, Russia

^d S.P. Korolev Rocket and Space Corporation “Energia”, Russia

Received 28 July 2014; revised 10 December 2014; accepted 11 December 2014

Available online 26 January 2015

Abstract

The paper proposes an experimental method of material inspection, which is based on digital processing of multi-frequency eddy current measurement data. The influences of various factors (conductivity, the gap between the sample surface and the sensor, the thickness of the sample) on the obtained hodographs are examined by taking the aluminum alloys for example, and the possibility of separation of various factors is analyzed. The results obtained are indicative of how much promise the proposed method offers for the inspection and testing of products made of aluminum alloys.

Copyright © 2015, China Ordnance Society. Production and hosting by Elsevier B.V. All rights reserved.

Keywords: Eddy current method; Material inspection; Digital signal processing; Aluminum alloy

1. Introduction

One of the nondestructive testing methods for metallic materials is an eddy current method [1] that makes it possible to estimate the internal structural state of the material [2], detect the surface and subsurface flaws [3], detect the fatigue cracks [4], and determine the crack location [5] and the geometrical parameters such as the thickness of metal sheet or dielectric coating on metal products [6]. The measured result of eddy current is determined by the combined action of a number of factors. Depending on the specific problem to be solved in non-destructive testing, it is necessary to isolate the effect of any one factor or group of factors. All the rest are in the number of the interfering factors and their effect should be excluded. The main factors affecting the eddy current measurements include electrical conductivity and magnetic

permeability that depend on the chemical composition and structure of the material, the geometric characteristics of a particular sample or products, the value of the gap between the probe and the surface of the object under control for overhead probes. In addition, the results of the measurements depend on the design peculiarities of the used probes [7] and measurement modes [8,9]. The efficiency of the eddy current inspection can be improved by reliably separating the effect of various factors.

The most informativity is achieved by using of the method of eddy current multi-frequency measurements, which are followed by the construction and analysis of hodographs of the “probe – specimen” system. Such hodographs plot the combined effect of almost all factors important for the inspection and testing of materials. The main problem with multi-frequency measurements is that their result depends on the combined action of a very large number of factors. Upon reaching sufficient precision, the experimental hodographs allow to separate the effect of various factors. One way of solving this problem is to employ new methods of digital

* Corresponding author. Institute of Strength Physics and Materials Science SB RAS, Russian Federation

E-mail address: eak@ispms.ru (E.A. KOLUBAEV).

Peer review under responsibility of China Ordnance Society.

processing of signals from an eddy current measuring system [10,11].

The present paper considers a method of deriving experimental hodographs, which provides a significant reduction in the measurement error and thus allows us to distinguish the factors affecting the properties under inspection. The investigation is performed on aluminum alloys widely used in modern engineering as constructional materials [12].

2. Experimental method

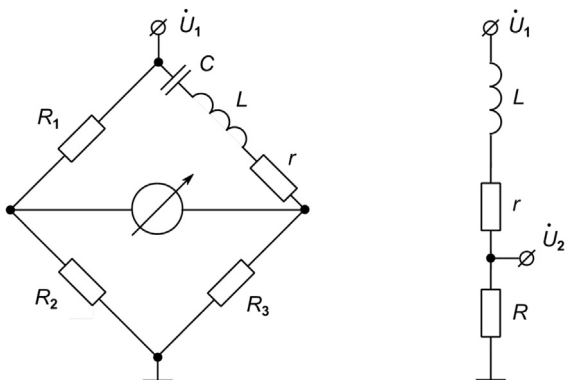
The eddy current testing helps us to determine the inductance and active resistance of the “eddy current probe – specimen” system. The tests are usually run with various bridge circuits and provide a smaller error in comparison to the direct measurement of system parameters. At the same time the bridge circuits make the measurement more difficult because of the necessity for constant bridge balancing. Besides, such balancing complicates considerably the test automation [13]. In this connection, the bridge measurements and direct detection of the probe impedance are conducted through the complex amplitudes of voltage and current. Both circuits are shown in Fig. 1.

Fig. 1(a) shows a resonant bridge circuit. The probe parameters are calculated by the formulae

$$L = \frac{1}{\omega^2 C} \tag{1}$$

$$r = \frac{R_1 R_3}{R_2}$$

where L and r are the inductance and active resistance of the eddy current probe, respectively; C is the capacitance of the capacitor; $R_1, R_2,$ and R_3 are the resistance values, at which the bridge is balanced; ω is the cyclic frequency of the sinusoidal input signal; and \dot{U}_1 in Fig. 1 is the complex input amplitude. Fig. 1(b) presents a circuit for the direct measurement of the probe impedance. In this case, the parameters are calculated by the formulae



(a) Resonant bridge circuit (b) Circuit for the direct measurement of impedance

Fig. 1. Circuits for the experimental measurements.

$$L = \frac{R U_{10}}{\omega U_{20}} \sin(\varphi_1 - \varphi_2) \tag{2}$$

$$r = R \left(\frac{U_{10}}{U_{20}} \cos(\varphi_1 - \varphi_2) - 1 \right)$$

where R is the resistance playing the role of the current-to-voltage converter; and U_{10} and φ_1 are the amplitude and initial phase of the input signal \dot{U}_1 , respectively; and U_{20} and φ_2 are the amplitude and initial phase of the signal \dot{U}_2 . All measurement results are shown as the hodographs plotted in the coordinates $\Delta X/X_0 - \Delta r/X_0$, where $\Delta X = \omega(L - L_0)$ is the variation in the reactive resistance of probe in the presence of the specimen, $\Delta r = r - r_0$ is the variation in the active resistance of probe in the presence of the specimen, X_0, L_0 and r_0 are the reactive resistance, inductance and active resistance of the probe without the specimen, respectively.

In both cases, a parametric probe of an encircling type is used. The probe presents a coil with 250 mm in length and 29 mm in effective diameter. A test specimen with round cross-section and longer than the coil is passed through the probe. Specimens are made of D16T duralumin and shaped to the rods with 400 mm in length and 22 mm in diameter. The measurements are made at fixed frequencies ranging from 200 Hz to 2 kHz. Each measurement for a given frequency is conducted with and without specimen for at least 10 times with the subsequent calculation of the probe parameters by Eqs. (1) and (2). The measurement results are represented in the hodographs as a series of experimental points, each of which corresponds to a specific frequency.

Along with the construction of experimental hodographs, the theoretical ones are calculated using the known values of probe characteristics, geometric parameters of specimens, and their specific electrical conductivity. The calculations are carried out by the formulas [1,3]

$$\frac{\Delta r}{X_0} = -2\eta\mu \text{Im} \left(\frac{I_1(y\sqrt{j})}{y\sqrt{j}I_0(y\sqrt{j})} \right) \tag{3}$$

$$\frac{\Delta X}{X_0} = 2\eta\mu \text{Re} \left(\frac{I_1(y\sqrt{j})}{y\sqrt{j}I_0(y\sqrt{j})} \right) - \eta$$

where μ is the relative magnetic permeability of the material; $\eta = (R_0/R_s)^2$ is the filling factor of the probe of effective radius R_s with a cylindrical specimen of radius R_0 ; $y = R_s \sqrt{\mu_0 \mu \sigma \omega}$ is the generalized eddy current parameter; σ is the specific electrical conductivity of the conductor; $\mu_0 = 4\pi \cdot 10^{-7}$ H/m is the magnetic constant; and $I_0(y\sqrt{j})$ and $I_1(y\sqrt{j})$ are the modified Bessel function of the first kind for zero and the first order [14], respectively. The calculation results of the theoretical hodographs are given as solid curves.

3. Digital signal processing in eddy current measurements

The digital processing of experimental signals was used to reduce the measurement error of complex voltage and current

amplitudes [15]. This processing consists in that the instantaneous signal values are approximated by the linear combination of the first three Walsh functions [16]

$$y(x) = b_0 \text{wal}(0,x) + b_1 \text{wal}(1,x) + b_2 \text{wal}(2,x) \quad (4)$$

where $\text{wal}(0,x)$, $\text{wal}(1,x)$ and $\text{wal}(2,x)$ are the first, second and third Walsh functions, respectively; $x = t/T$ is the relative time; and T is the signal period. The coefficients in Eq. (4) are as follows

$$b_0 = U_0; b_1 = \frac{2U_m}{\pi} \cos \varphi_0; b_2 = \frac{2U_m}{\pi} \sin \varphi_0 \quad (5)$$

where U_0 is the constant bias voltage; U_m is the harmonic signal amplitude; and φ_0 is the initial phase. Such a series describes very roughly the harmonic signal and however its coefficients contain all necessary information on the searched parameters. Values of b_0 , b_1 and b_2 are found in processing of the experimental data by the least squares method. The criterion for the optimal choice of weighting factors is the minimum of the objective function

$$S(b_0, b_1, b_2) = \sum_{i=1}^N \left[\sum_{n=0}^2 b_n \text{wal}(n, X_i) - Y_i \right]^2 \quad (6)$$

where X_i and Y_i in calculating the Walsh functions take on $+1$ or -1 , which leads to the sign reversal in summation.

The proposed approach is validated in three different tests with different measuring circuits. The derived results are shown in Fig. 2. In the first test, the probe impedance is determined using a resonant bridge circuit (Fig. 1(a)), and the test values are illustrated as the points in Fig. 2(a), where the points represent the mean values of the relative driving-point impedances, and the mutual intersection of two lines at a point indicates the standard error of these values. In the second and third tests, the impedance is directly measured by a

voltmeter and phase meter. Fig. 2(b) shows the immediate results of such measurements while Fig. 2(c) exhibits the data of experimental signals processed by the Walsh functions. In addition, the solid curves in these figures represent the theoretical hodographs calculated by Eq. (3).

The comparison of the hodographs in Fig. 2(a) and (b) shows that the experimental points for the bridge circuit are placed closer to the theoretical curve and have a much smaller error. The minimum measurement error is found in Fig. 2(c), where the experimental points lie on the theoretical curve. Thus, the method combining the direct measurement of probe impedance and digital signal processing using Walsh functions provides both high measuring accuracy competitive with that of bridge circuits and ease of its implementation necessary for use in an automated measuring and computing complex.

4. Test results for aluminum alloys

Inspected products made of aluminum alloys can have different dimensions and shapes, which narrows significantly the field of application of encircling probes under actual operating conditions. Therefore further measurements are carried out using a parametric probe. The probe presents a coil placed into a ferrite magnetic core with semi-shell structure made of manganese–nickel ferrite with relative initial magnetic permeability $\mu = 2000$. The diameter of the probe is 15 mm. The choice of this design was driven by the fact that the signal received from the probe at the same time dependent on several factors, such as electrical conductivity of gap and sheet thickness), which reveals the possibility of the proposed method for separating the influences of various factors. Measurements were carried out at frequencies from 100 Hz to 6.4 kHz, which provides a reliable separation of hodograph lines for probe mentioned above. The measurements are performed with the use of an automated measuring and computing complex by using the above-described method to directly determinate the probe impedance and the Walsh functions for digital signal processing.

The block scheme of the eddy current measuring system is shown in Fig. 3. A harmonic signal supplied by generator 1 is fed to an electric circuit consisting of series-connected eddy current parametric probe (L and r) and resistance R ($R = 50$ Ohms). Analog-to-digital converters 2 and 3 digitize the voltages U_1 and U_2 , respectively, and the digitized data are transmitted to the control computer, which is also used to set the operating mode of the generator, by communication channel 4. Fig. 4 shows the measuring unit of eddy current measuring system together with probe superimposed on a controlled sample.

To determine the capacity of the proposed diagnostic method, the effects the size of the gap between the sheet surface and the contact sensor, and the thickness and conductivity of the material sheet on eddy current measurement results were studied. The test specimens present the flat sheets of AMg5 aluminum alloy from 5 to 10 mm in thickness. The inspection possibilities depend on the effect of such factors as the gap width between the probe and the sheet surface, sheet

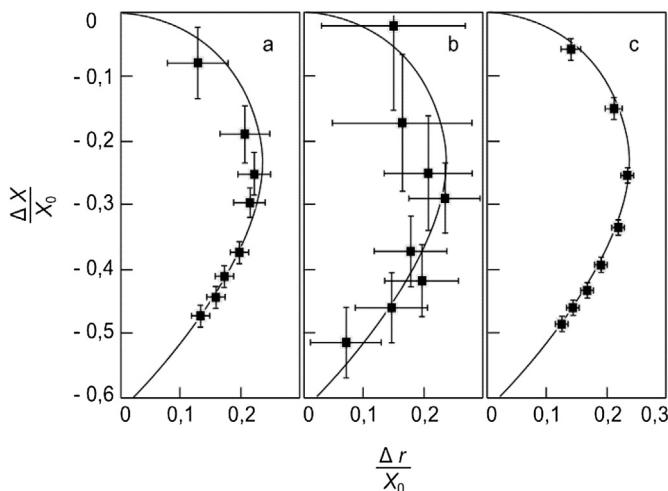


Fig. 2. Experimental hodographs of different measuring circuits, (a) Bridge circuit (b) Direct measurement of impedance (c) Direct measurement of impedance and digital signal processing.

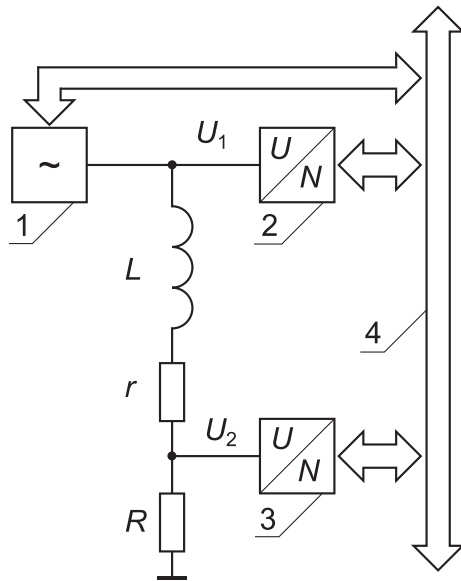


Fig. 3. Block scheme of the measuring unit of the eddy current measuring system.

thickness, and electrical conductivity of the material. The test results are shown as the points on the experimental hodographs in Fig. 5 (for convenience, in comparing the hodographs, the points are connected by dotted lines found by interpolation).

Fig. 5(a) shows the hodograph for different gap width (being almost zero for points 1, and being 160 μm for points 2). The hodograph lines are seen to noticeably shift relative to each other. The curves diverge strongly in their lower portions corresponding to high frequencies, which are caused by the small thickness of the skin layer and the consequent stronger effect of the gap.

Fig. 5(b) presents the measured results of the specimens made of aluminum alloys with different electrical conductivities (for points 1, $\sigma = 15.7$ MS/m, and for points 2, $\sigma = 19.5$ MS/m). Different conductivities are explained by various chemical compositions of alloys (various concentrations and types of alloying elements). Referring to Fig. 5(b), both groups of points fall on the same curve, and in so doing



Fig. 4. Exterior view of the measuring unit of eddy current measuring system.

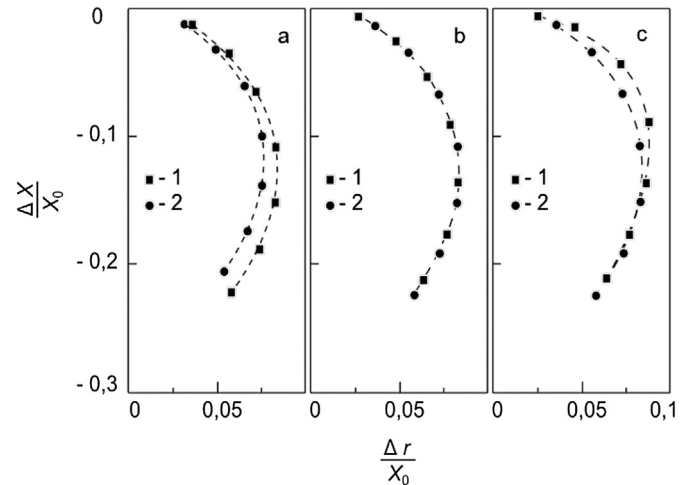


Fig. 5. Experimental hodographs for aluminum alloys. (a) Gap effect: 1, lack of a gap for points, 2, 160 μm gap for points; (b) Effect of electrical conductivity: 1, $\sigma = 15.7$ MS/m, 2, $\sigma = 19.5$ MS/m; (c) Effects of specimen thickness and electrical conductivity: 1, $h = 5$ mm, $\sigma = 15.7$ MS/m, $h = 8.7$ mm, 2, $\sigma = 19.5$ MS/m.

the points corresponding to the same frequencies are shifted relative to each other along this curve. This shift of points is due to the fact that their positions in the hodograph line are governed by the generalized eddy current parameter proportional to the product of specific conductivity and frequency $\sim \sqrt{\sigma\omega}$.

Fig. 5(c) illustrates the simultaneous effect of both factors, namely, the thickness of the specimen and the conductivity of the material (for points 1 the sheet thickness $h = 5$ mm and the specific conductivity $\sigma = 15.7$ MS/m, for points 2 $h = 8.7$ mm and $\sigma = 19.5$ MS/m). The hodographs for specimens with different thicknesses are seen to differ in shape, which is due to the divergence of their upper portions corresponding to low frequencies. This divergence is governed by the effect of the skin layer, whose thickness at low frequencies is comparable with the sheet thickness. The lower portions of the hodographs describing high frequencies match due to the small thickness of the skin layer the sheet thickness has almost no effect on the position of the hodograph line. At the same time, despite the curve coincidence the corresponding experimental points are significantly shifted relative to each other along the hodograph line due to different conductivity.

It should be noted that the suppression of interfering factors is extremely difficult since the eddy current techniques are based on measurements at one fixed frequency. As a rule, the interfering factors are suppressed by time-consuming procedures for selecting the measurement mode. Thus, in the resonant eddy current inspection, a measurement frequency is selected experimentally on the left slope of the resonance curve, which allows reducing the influence of the gap width to 100 microns during inspection of non-ferrous metals [1]. A weakening of the influence of larger gap (up to 200 microns) provides an eddy current technique based on measurement of the variable phase of harmonic signal in eddy current probe. In this case, it needs to carefully select the initial complex

amplitude of the reference signal. The proposed method does not have these disadvantages.

5. Conclusions

The proposed approach based on multi-frequency measurements and digital processing of the recorded signals allows to identify successfully and to separate the influence of various factors which are very important for eddy current inspection (sample thickness, gap between probe and sample, change in electric conductivity). This indicates the prospects of this approach for the inspection of materials and products made of aluminum alloys.

Acknowledgment

The work has been supported by Program for Basic Scientific Research of the State Academies of Sciences for 2013–2020 and the RF Ministry of Education and Science (Contract No. 02.G25.31.0063) in the framework of RF Government Order No. 218.

References

- [1] Nondestructive testing: Handbook: In 8 volumes / Edited by V.V. Klyuev / Volume 2, Moscow: Mashinostroenie, 2003, 688 p.
- [2] Polyakov VV, Egorov AV. Eddy current testing of specific electrical conductivity and magnetic permeability of products from magnetic soft materials. *Defectoscopia* 1992;12:78–80.
- [3] Dorofeev AL, Kazamanov YuG. Electromagnetic testing. Moscow: Mashinostroenie; 1980.
- [4] Sasi B, Rao BPC, Jayakumar T, Raj Baldev. Development of eddy current test procedure for non-destructive detection of fatigue cracks and corrosion in rivets of air-intake structures. *Def Sci J* 2009;59(2):106–12.
- [5] Song Zenglu, Yamada Tsutomu, Shitara Hideki, Takemura Yasushi. Detection of damage and crack in railhead by using eddy current testing. *J Electromagn Anal Appl* 2011;3:546–50.
- [6] Polyakov VV, Egorov AV. Magnetic and electrical characteristics of porous ferromagnets. *Dok Akad Nauk* 1995;344(4):479–80.
- [7] Golovnev IF, Golovneva EI, Merzhievsky LA, Fomin VM. Defect generation as a phenomenon of structure self-organization under external loads. *Phys Mesomech* 2013;16(4):294–302.
- [8] Garcia-Martín J, Gómez-Gil J, Vázquez-Sánchez E. Non-destructive techniques based on eddy current testing. *Sensors (Basel)* 2011;11(3):2525–65.
- [9] Bashtannikov LA, Bondarenko VI, Sebko VP, Tyupa VI. Determination of electromagnetic characteristics of the material of solid cylindrical products. *Defectoscopia* 1980;8:5–9.
- [10] Polyakov VV, Golovin AV, Egorov AV, Utemesov MA. Correlation of acoustic and physico-mechanical characteristics of porous materials. *Defectoscopia* 1994;9:48–50.
- [11] Kucheryavskii SV, Polyakov VV. Multivariable data analysis techniques for the study of the material structure. *Zavod Lab Diag Mat* 2007;73(8):32–6.
- [12] Shang-kun Ren, Da-peng Sun. Studies of eddy current testing on nuclear power steam generator tube based on finite element simulation. In: 2nd international conference on materials, mechatronics and automation lecture notes in information technology, vol. 15; 2012. p. 217–22.
- [13] Egorov AV, Polyakov VV, Ivakov SV. A measuring and computing complex for the eddy current detection of specific conductivity and magnetic permeability. *Polzunov Vest* 2010;2:129–31.
- [14] Korenev BG. Introduction to the theory of Bessel functions. Moscow: Nauka; 1971.
- [15] Max J. Méthodes et techniques de traitement du signal et applications aux mesures physiques. Paris: Masson; 1987.
- [16] Zalmanson LA. Fourier, Walsh, and Haar transforms and their application in management, communication, and other fields. Moscow: Nauka; 1989.